MIXED CONVECTION AND STRATIFICATION PHENOMENA IN A HEAVY LIQUID METAL POOL

Mariano Tarantino[1*], Daniele Martelli[2], Gianluca Barone[2], Ivan di Piazza[1], Nicola Forgione[2]

1. Italian National Agency for New Technologies, Energy and Sustainable Economic Development, C.R. ENEA Brasimone, Italy.
2. Dipartimento di Ingegneria Civile e Industriale, University of Pisa, Largo Lucio Lazzarino, 1-56100 Pisa Italy

* Corresponding author. E-mail: mariano.tarantino@enea.it

HIGHLIGHTS

- A STH/CFD coupling tool is developed for thermal-hydraulics analyses.
- Explicit numerical coupling scheme are implemented.
- A preliminary coupling tool assesment is presented.
- Natural, assisted circulation and ULOF tests are simulated.

Abstract

This work deals with an analysis of the first experimental series of tests performed to investigate mixed convection and stratification phenomena in CIRCE HLM large pool. In particular, the tests concern the transition from nominal flow to natural circulation regime, typical of Decay Heat Removal (DHR) regime. To this purpose the CIRCE pool facility has been updated to host a suitable test section in order to reproduce the thermal-hydraulic behaviour of a HLM pool-type reactor. The test section basically consists of an electrical bundle (FPS) made up of 37 pins arranged in an hexagonal wrapped lattice with a pitch diameter ratio of 1.8. Along the FPS active length, three sections were instrumented to monitor the heat transfer coefficient along the bundle as well as the cladding temperatures at different ranks of the sub-channels. This paper reports the experimental data as well as a preliminary analysis and discussion of the results, focusing on the most relevant tests of the campaign, namely Test I (48 h) and Test II (97 h). Temperatures along three sections of the FPS and at inlet and outlet sections of the main components were reported and the Nusselt number in the FPS sub-channels was investigated together with the void fraction in the riser. Concerning the investigation of in-pool thermal stratification phenomena, the temperatures in the whole LBE pool were monitored at different elevations and radial locations. The analysis of experimental data obtained from Tests I and II underline the occurrence of thermal stratification phenomena in the region placed between the outlet sections of the HX and the DHR respectively. After the transition to natural circulation, for both tests, this region with temperature stratification moves downwards starting at the exit section of the DHR-system, while upper and lower vessel regions show a uniform temperature.

1. Introduction

The European Union produces 30% of its electricity via nuclear fission in so-called second and third generation light water reactors (LWR) and, for some countries, the nuclear fission represents part of their sustainable energy mix (Sustainable Nuclear Energy Technology Platform, 2010). Safety and waste issues have to be considered and managed carefully at the international level. In particular, nuclear waste must be managed appropriately. Currently, the adapted approach is geological disposal, possibly preceded by used fuel reprocessing. This latter depends on fuel cycle choices and waste management policies of an individual country. In any case, the time scale involved in geological disposal exceeds that of the history of accumulated technological knowledge. As a result, geological disposal of nuclear waste does suffer from public acceptance problems.

In various studies, partitioning and transmutation (P&T) in critical and/or sub-critical fast spectrum transmuters has been identified as a way of reducing the volume and decay time of nuclear waste (Seventh Framework Programme FP7, 2014). This reduces the required monitoring period to technologically feasible and manageable time scales. Also in the framework of the GEN IV initiative this approach has already been put forward.

On a European level a collaborative effort supported by the European Commission (EC) and European research institutes and industries was started to bring advanced fuel cycles and the P&T strategy together, in order to investigate its economic and technical feasibility (Sustainable Nuclear Energy Technology Platform, 2010). The exploratory research done in the field and the launch of the Sustainable Nuclear Energy Technology Platform (SNE-TP) in 2007 lead to a joined effort from the European nuclear fission research community to issue a Strategic Research and Innovation Agenda (SRIA) that describes the roadmap towards sustainable nuclear fission energy.

SNE-TP community identifies sodium fast reactor technology as the reference but also highlights the need for the development of an alternative track with lead or gas cooling. In addition, the need for R&D activities in support of accelerator driven systems (ADS) was stressed to allow the demonstration of ADS technology by the construction of the first ADS Demo facility, (MYRRHA, De Bruyn et al., 2007).

Regarding alternative fast reactor technologies as described in the SRIA (Sustainable Nuclear Energy Technology Platform, 2014), lead cooled fast reactor (LFR) systems are very promising in meeting the Gen IV requirements in terms of sustainability, economics, safety and reliability and proliferation resistance & physical protection. This assessment is based on inherent properties of the reactor coolant and on basic design choices.

In the European Strategic Nuclear Infrastructure Initiative (ESNII) implementation plan, the roadmap for the development, design construction and operation of a lead cooled fast reactor is put out. The conceptual design of a LFR Demonstrator (ALFRED) is foreseen (Alemberti et al., in press).

Since the Lead-cooled Fast Reactor (LFR) has been conceptualized in the frame of GEN IV International Forum (GIF), ENEA is strongly involved on the HLM technology development.

Currently ENEA has implemented large competencies and capabilities in the field of HLM thermal-hydraulics, coolant technology, material for high temperature applications, corrosion and material

protection, heat transfer and removal, component development and testing, remote maintenance, procedure definition and coolant handling (Foletti et al., 2006 and Cinotti et al., 2012).
In this frame the CIRCE pool facility (CIRCulation Eutectic) was refurbished to host a suitable test section able to simulate the thermal-hydraulic behaviour of the primary system in a HLM cooled pool reactor . In particular, a fuel pin bundle simulator (FPS) was installed in the CIRCE pool (Bandini et al., 2011, Tarantino et al. 2011). It was designed with a thermal power of about 1 MW and a linear power up to 25 kW/m, relevant values for a LMFR.
The aim of this experimental campaign performed in CIRCE facility arranged with the Integral Circulation Experiment (ICE) configuration is to characterize the phenomena of mixed convection and stratification in a liquid metal pool in a safety relevant situation.
Most of the works available in literature, concerning natural circulation phenomena of interest in the nuclear field, deal with results obtained using water or sodium as working fluids (Ishitori et al. 1987 and Watanabe et al., 1994). Furthermore, most of them neglect the thermal stratification that is instead considered one of the most important topics in the study of Generation IV reactors for increasing reactor safety and its structural integrity. Because of an accidental scenario, the reactor is scrammed, and assuming the total loss of the pumping system, the coolant flow rate reduces and large temperature variation takes place causing thermal stratification phenomena inside the pool. A stiff vertical temperature gradient may induce significant thermal loads on the structure in addiction to existing mechanical loads. Moreover, due to the instability (with respect to the position) of the stratification interface low frequency oscillations with large amplitude are generated. Since the thermal conductivity of HLM is 10-100 times higher than that of water (for lead at 450 °C the thermal conductivity is about 17 W/m K) temperature fluctuations are transmitted with low attenuation to the structure, leading to thermal cycle fatigue on the surface of the structure materials
To this end, the transition from nominal flow full power conditions to natural circulation decay heat removal conditions was explored, investigating mixing and stratification in large pool. In order to investigate pool thermal-hydraulics and provide experimental data for the validation of CFD models, the on-set and stabilization of the DHR flow path was monitored by means of a suitable instrumentation. Several thermocouples were used in the 3D domain to map the thermal stratification during the transient. Due to the integral nature of the facility, the tests will also be valuable for the verification of the system codes in mixed-convection conditions or to asses coupled STH/CFD methods (Tarantino et al., 2006).
Finally, the experiments in mixed and natural convection conditions, carried out in the CIRCE facility, will provide data for code-to-experiment comparison.

List of acronyms

ALFRED	Advanced Lead Fast Reactor European Demonstrator
ADS	Accelerator Driven System
CFD	Computational Fluid Dynamics
CIRCE	CIRColazione Eutettico
CR	Research Centre
DHR	Decay Heat Removal
EFIT	European Facility for Industrial Transmutation

FP7	7th Framework Programme
FPS	Fuel Pin bundle Simulator
EC	European Commission
ENEA	Italian National Agency for New Technologies, Energy and Sustainable Economic Development
ESNII	European Strategic Nuclear Infrastructure Initiative
GEN-IV	GENeration Four
GIF	Generation Four International Forum
HLM	Heavy Liquid Metal
HX	Heat eXchanger
IVCS	Insulation Volume Cooling System
LBE	Lead Bismuth Eutectic alloy
LFR	Lead cooled Fast Reactor
LMFR	Liquid Metal Fast Reactor
LWR	Light Water Reactor
MHYRRA	Multi-purpose hybrid Research Reactor for High-technology Applications
Nu	Nusselt Number
P&T	Partitioning and Transmutation
PLOF	Protected loss of flow
PLOHS	Protected loss of heat sink
Pe	Peclet Number
Re	Reynolds Number
SG	Steam Generator
SNE-TP	Sustainable Nuclear Energy – Technology Platform
SRIA	Strategic Research and Innovation Agenda
THINS	Thermal-Hydraulics of Innovative Nuclear Systems
TC	Thermocouple
XT-ADS	Experimental Accelerator Driven System

2. The experimental facility

2.1 CIRCE facility and ICE test section

CIRCulation Eutectic (CIRCE) is a pool type facility consisting of a cylindrical vessel (Main Vessel S100) filled with about 70 tons of molten Lead-Bismuth Eutectic (LBE) with argon cover gas and recirculation system, LBE heating and cooling systems, several test sections welded to and hung from bolted vessel heads for separate-effects and integral testing and auxiliary equipment for eutectic circulation (Turroni et al. 2001, Benamati et al. 2005, Tarantino and Scadozzo 2006, Bandini et al. 2011).

The facility is completed by a LBE storage tank (S200), a small LBE transfer tank (S300) and a data acquisition system. During the loading operations, the LBE is gradually transferred from the storage tank (S200) to the S300 vessel. Then, by pressurization of the S300 cover gas, the liquid metal gradually fills the test vessel (S100) from the bottom.

The main vessel S100 consists of a vertical vessel 8500 mm in height, connected by gates to the other vessels. It is externally equipped with electrical heating cables, installed at the bottom and on the lateral surface. This heating system operates in a temperature range of 200-400°C.

A skimming line and a passive pressure safety system are also present in the main vessel, in order to guarantee the LBE top level and to prevent accidental overpressure. The S100 main parameters are summarized in the work of Tarantino et al., 2011.

The Integral Circulation Experiment (ICE) test section is contained in the S100 main vessel and it was conceived to reproduce thermal-hydraulic behaviour of the Experimental Accelerator Driven System (XT-ADS) and European Facility for Industrial Transmutation (EFIT) primary system (Mansani 2005, Barbensi and Corsini 2006, Giraud 2006, Artioli 2006,Van den Eynde 2007).

Figure 1 shows the ICE test section placed inside the CIRCE main vessel S100 (for a detailed description of the test section see Tarantino et al., 2011)

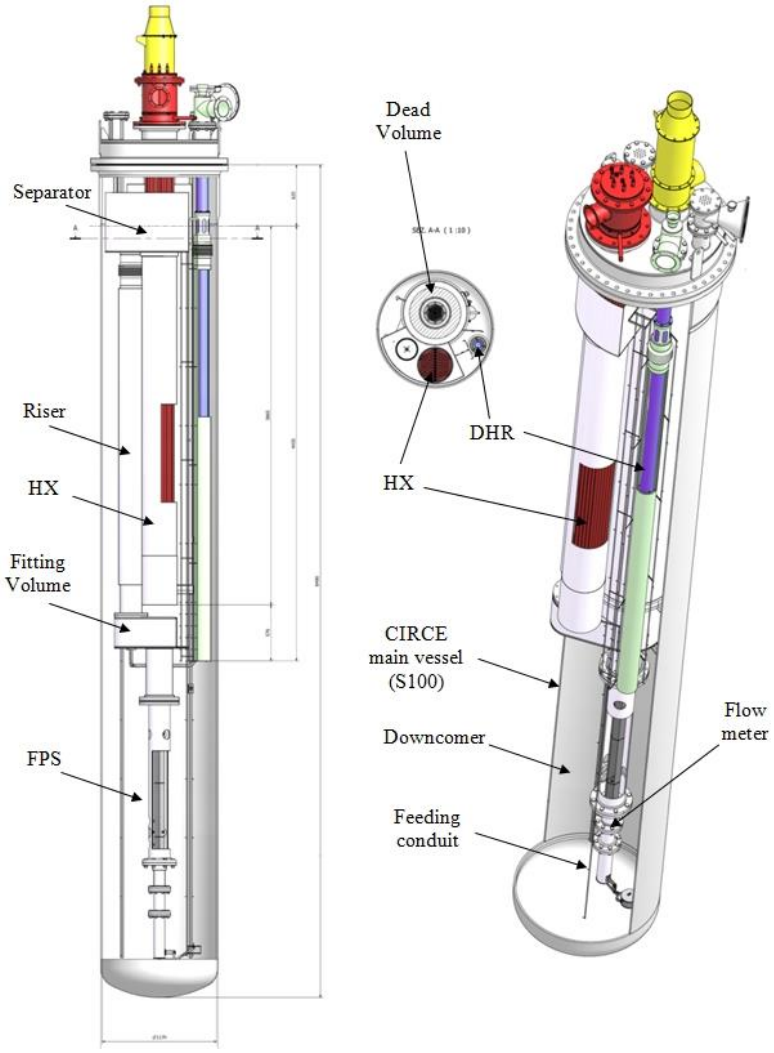

Figure 1: ICE Test section

2.2 CIRCE-ICE instrumentation

All the thermocouples installed in the CIRCE facility are *N* type with isolated hot junction. For those installed in the FPS sub channels having a diameter of 0.5 mm the accuracy is ±0.1°C, while the accuracy of the others is ±1°C. The calibration and accuracy of the Venturi flow meter were deeply investigated in a previous experimental campaign (Ambrosini et al. 2004, Agostini et al. 2005). In particular, the relative error for an indirect evaluation of the mass flow rate due to an uncertainty of 1 mm of lead-bismuth on the differential pressure corresponds to a relative error of about 25% for mass flow rate measurements lower than 50 kg/s (Agostini et al. 2005).

2.2.1 FPS instrumentation

The ICE heat source consists of an electrical pin bundle with a nominal thermal power of about 800 kW. It consists of 37 electrical pins arranged in a wrapped hexagonal lattice. The relative position between the pin bundle and the wrapper was fixed by three spacer grids placed along the axis of the component. The upper and lower spacer grids were placed at the interface between the active and non-active length of the electrical pins to enclose the mixing zones. The middle spacer grid was placed in the middle section of the bundle's active length. From a hydraulic point of view, the FPS assures the overall LBE flow rate runs along the HS, without any by-pass. In Table 1 the main data of the HS are summarized.

Table 1: HS main parameters

Parameter	***Value***
Number of pins n	37
Pin outer diameter ϕ	8.2 mm
Power of a pin	25 kW
Pin wall heat flux	1 MW/m^2
Pitch to diameter p/ϕ	1.8
Active Length	1 m
l' (wrapper side length)	55.4 mm
H' (wrapper width)	96 mm

The LBE temperature at the FPS entrance was measured by three thermocouples with a diameter of 3 mm (named TC-FPS-31, 32, 33, see Figure 2). The LBE temperature at the FPS exit section was measured by three thermocouples (TC-FPS-37, 38, 39) of the same type of those at the entrance.

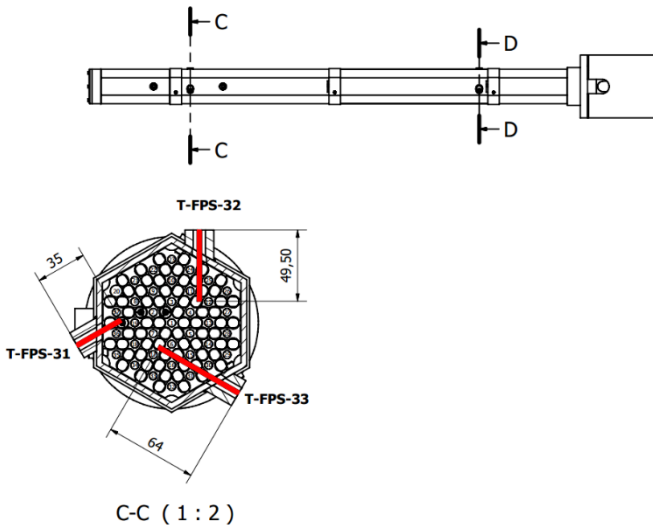

Figure 2: Thermocouples at the FPS entrance

Regarding the positioning of the thermocouples along the FPS active zone, four different sections were monitored (see Figure 3):

- Section 1 (Figure 4): 20 mm upstream the middle spacer grid. In this section three different sub-channels were instrumented. In each sub-channel both pin clad and LBE bulk temperatures were measured (TC-FPS-01 to 09).
- Section 2 (Figure 5): on the matching surface between the middle spacer grid and the fuel pins. In this section the pin clad temperature for the three sub channels identified at section 1 was monitored (TC-FPS-10 to 14), aiming at the hot spot factor evaluation due to the installation of the spacer grid itself.
- Section 3 (Figure 6): 60 mm upstream of the upper spacer grid. In this section the same sub-channels have been identified in sections 1 and 2 for temperature measurements at the upper height of the bundle. In each sub-channel both pin clad and LBE bulk temperatures were measured (TC-FPS-16 to 24).
- Section 4 (Figure 7): 60 mm downstream of the lower spacer grid. In this section the LBE bulk temperature was measured in each sub-channel (TC-FPS-28 to 30).

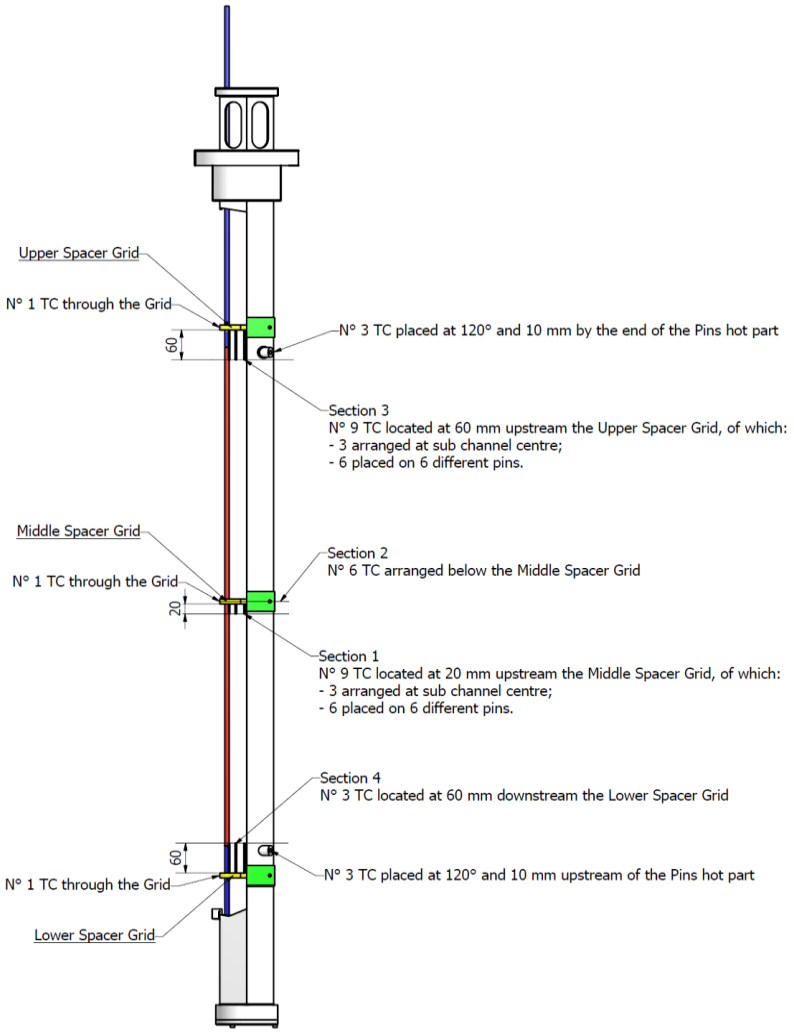

Figure 3: FPS sketch and measurement sections

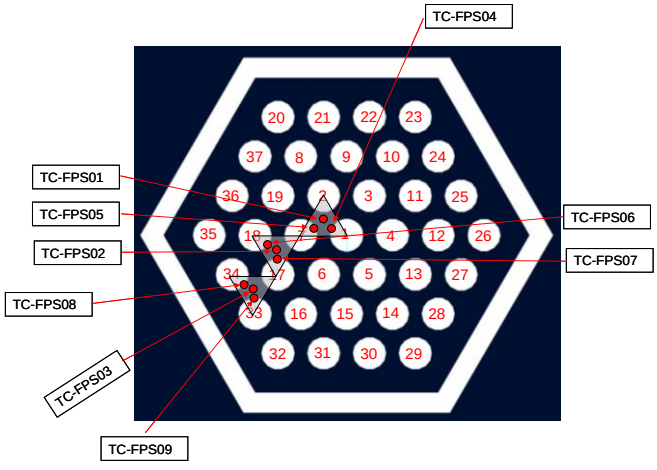

Figure 4: Section 1, sub-channels instrumented

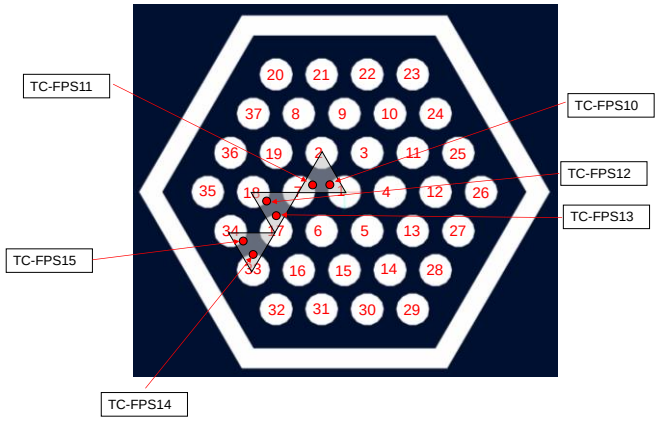

Figure 5: Section 2, sub-channels instrumented

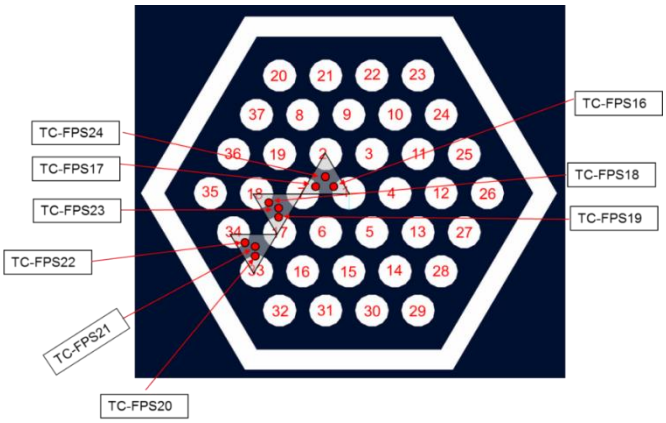

Figure 6: Section 3, sub-channels instrumented

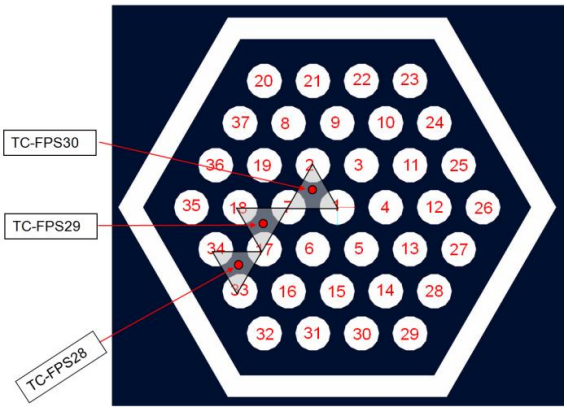

Figure 7: Section 4, sub-channels instrumented

Thermocouples used in the four previously defined sections have a diameter of 0.5 mm. In Figure 8 the technical solution adopted for the positioning and fixing of the thermocouples is shown.

Figure 8: TCs positioning and fixing

2.2.2 RISER and HX instrumentation

The LBE heated by the FPS flows through the fitting volume into the riser; here temperatures were measured using TCs with a diameter of 3 mm disposed at the entrance section (T-TS-01 to 03 and at the exit section before the separator (T-TS-04 to 06).

From the riser exit, the LBE flows through the Separator into the HX shell, where temperatures at the entrance section were measured by three TCs placed at 120°, 30 mm from the bottom of the Separator (T-SG-01 to 03).

Sub-channel temperature measurements were taken on a plane placed 30 mm above the lower grid, according to the scheme shown in Figure 9 (T-SG-04 to 12).

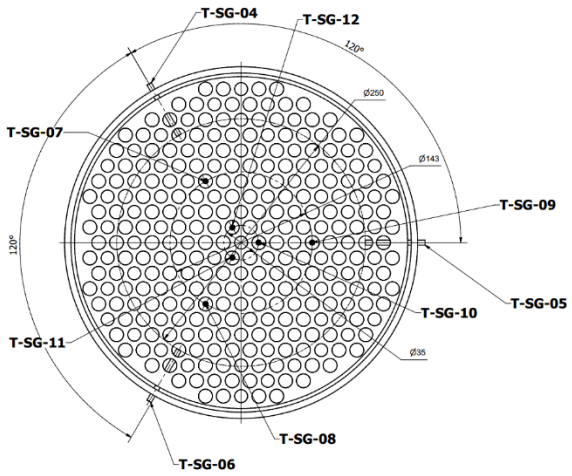

Figure 9: HX Sub-channels TCs configuration

Temperatures at the HX exit were measured with six TCs (T-SG-13 ... 18) placed at 60° each and at 100 mm before the HX skirt exit (see Figure 10).

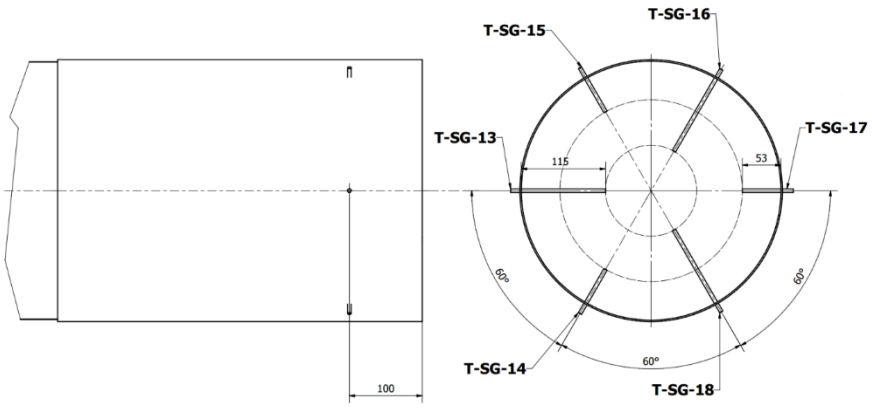

Figure 10: TCs configuration at the HX exit

2.2.3 DHR instrumentation

The Decay Heat Removal system is activated to reproduce behaviour in the case of an accidental event with total loss of HX heat sink and consequent reactor scram (Bandini et al. 2011). It consists of a bayonet tubes cooled by low pressure air. The velocity of the air flowing through the inner tube was measured by a hot wire anemometer placed in the tube at the entrance of the DHR and the mass flow rate was derived using the calibration curve given by the manufacturer. The air temperature was measured at the entrance and at the exit section of the secondary circuit, as shown in Figure 11. Regarding the primary circuit (LBE side), temperatures at the inlet of the DHR were measured by six TCs with a diameter of 3 mm, placed in the slots at the entrance of the DHR shell according to Figure 12 (T-DHR-07 to 12).

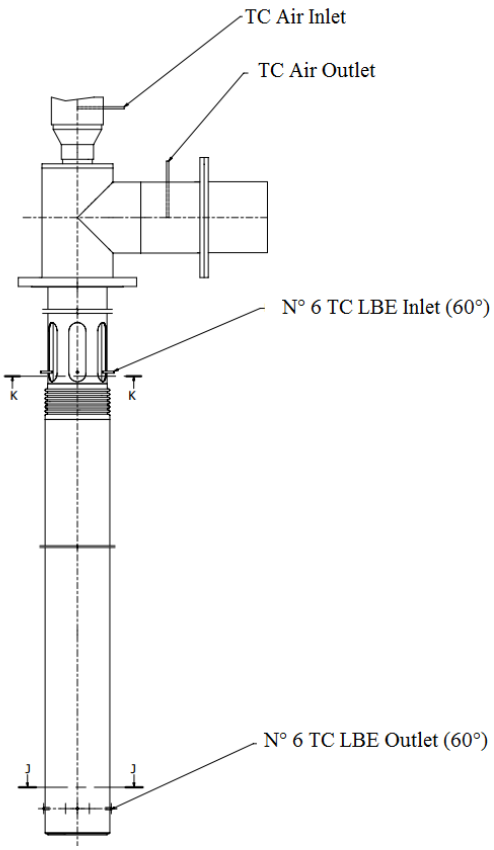

Figure 11: Sketch of TCs placed in the DHR

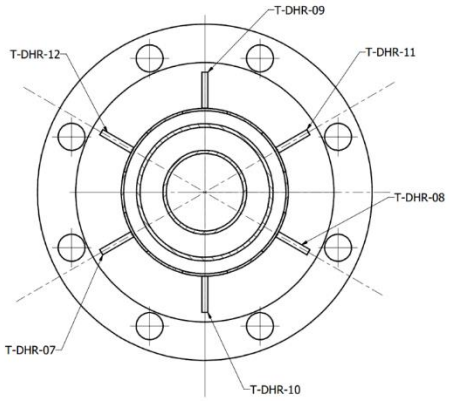

Figure 12: TCs configuration at the DHR inlet

The LBE temperature at the exit of the DHR was measured at 60 mm from DHR skirt outlet section, by six TCs with a diameter of 3 mm (T-DHR-01 to 06) placed at 60° according to the scheme shown in Figure 13and Figure 14.

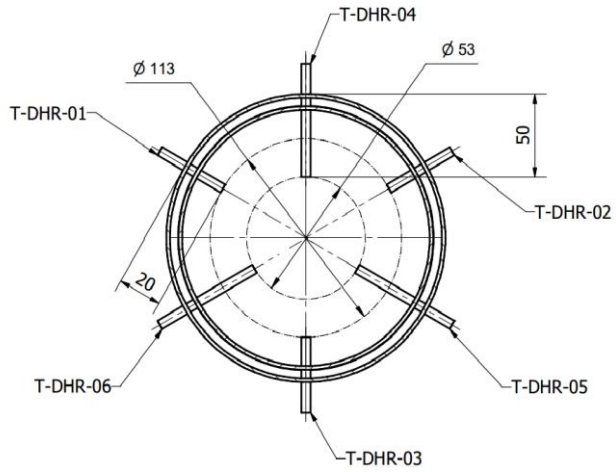

Figure 13: TCs configuration at the DHR outlet

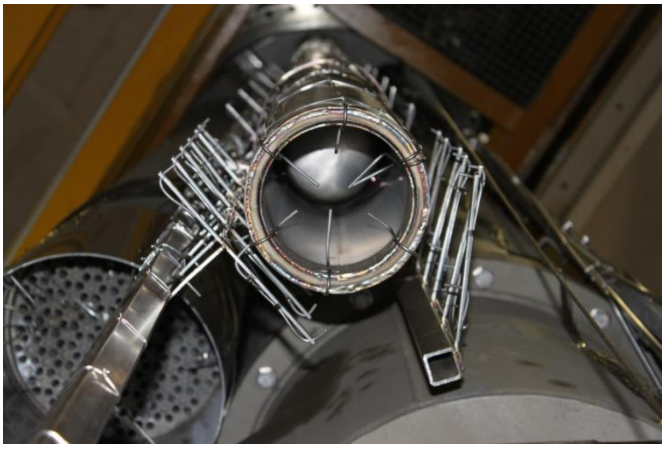

Figure 14: TCs at the DHR outlet

2.2.4 LBE pool instrumentation

Several TCs were installed in the LBE pool in order to investigate mixing and stratification phenomena. For that purpose, vertical rods for the TCs attachment have been installed into the pool fixing the TCs at 17 different elevations for a total of 119 TCs with a diameter of 3 mm (T-MS-01 to 119). In particular, according to Figure 15 and Figure 16, TCs on lines *A*, *H* and *I* allow measurements from the bottom side of the test section up to the FPS entrance, while TCs on lines *B*, *C*, *D*, *E*, *F* and *G* allow measurements up to 600 mm below the exit of the DHR.

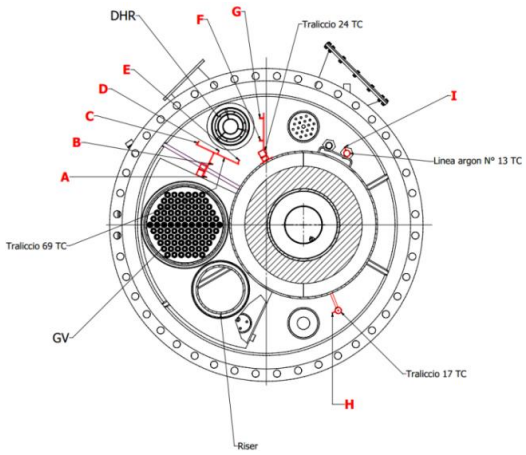

Figure 15: Arrangements of the vertical support for the TCs

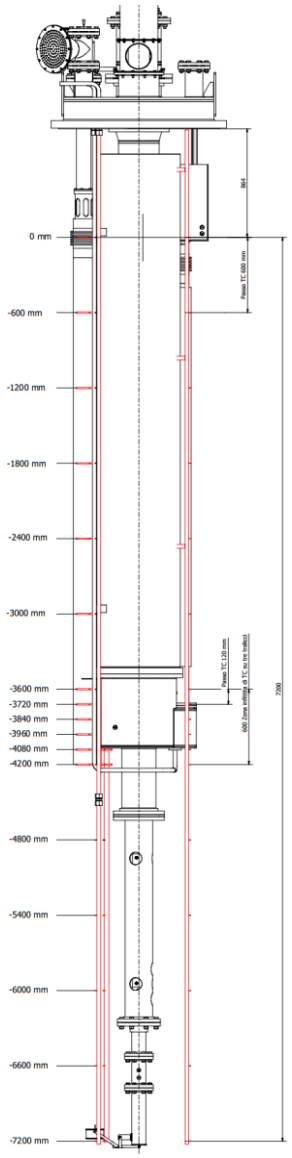

Figure 16: TCs vertical positioning

In Table 2 all the TCs installed inside the LBE pool are reported specifying their name and vertical position.

Table 2: **TCs placed inside the LBE pool**

TC	*Vertical support*	*Vertical position [mm]*
T-MS-01 to T-MS-05	A,B,C,D,E	0
T-MS-06 to T-MS-09	F,G,H,I	
T-MS-10 to T-MS-14	A,B,C,D,E	-600
T-MS-15 to T-MS-18	F,G,H,I	
T-MS-19 to T-MS-23	A,B,C,D,E	-1200
T-MS-24 to T-MS-27	F,G,H,I	
T-MS-28 to T-MS-32	A,B,C,D,E	-1800
T-MS-33 to T-MS-36	F,G,H,I	
T-MS-38 to T-MS-41	A,B,C,D,E	-2400
T-MS-42 to T-MS-45	F,G,H,I	
T-MS-46 to T-MS-50	A,B,C,D,E	-3000
T-MS-51 to T-MS-54	F,G,H,I	
T-MS-55 to T-MS-59	A,B,C,D,E	-3600
T-MS-60 to T-MS-63	F,G,H,I	
T-MS-64 to T-MS-68	A,B,C,D,E	-3720
T-MS-69 to T-MS-71	F,G,H	
T-MS-72 to T-MS-76	A,B,C,D,E	-3840
T-MS-77 to T-MS-79	F,G,H	
T-MS-80 to T-MS-84	A,B,C,D,E	-3960
T-MS-85 to T-MS-86	F,G,H	
T-MS-88 to T-MS-92	A,B,C,D,E	-4080
T-MS-93 to T-MS-95	F,G,H	
T-MS-96 to T-MS-100	A,B,C,D,E	-4200
T-MS-101 to T-MS-104	F,G,H,I	
T-MS-105 to T-MS-107	A,H,I	-4800
T-MS-108 to T-MS-110	A,H,I	-5400
T-MS-111 to T-MS-113	A,H,I	-6000
T-MS-114 to T-MS-116	A,H,I	-6600
T-MS-117 to T-MS-119	A,H,I	-7200

3. Experiment description

The main objective of the CIRCE-ICE experiment is the characterization of mixed convection and stratification phenomena in a heavy liquid metal pool in safety relevant situations. The performed tests were aimed at reproducing a Protected Loss Of Heat Sink (PLOHS) with Loss Of Flow (LOF), simulating the total loss of the secondary circuit, the consequent reactor scram and activation of DHR system to remove the decay heat power (5-7% of the nominal value). In the CIRCE-ICE facility the transition from nominal condition (forced circulation) to natural circulation was performed reducing the thermal power generated in the HS, stopping the argon injection into the riser, cutting off the main HX

and activating the DHR heat exchanger. The main nominal parameters that define the accidental scenario experimentally reproduced are summarized in Table 3.

Table 3: Nominal parameters for the experimental campaign

Nominal Steady State	**PLOH+LOF transient**
HS Thermal Power :600-800 kW	Isolation of the main HX (isolating the feed water)
HLM flow rate: 55-65 kg/s (by gas lift)	Core "scram" at 20-50 kW (decay power)
ΔT along the HS: 100°C	Start-up of the DHR-system ($\dot{m} = 0.3$ kg/s)
Average velocity into the HS:1m/s	"Main pump" turn-off (the gas injection is interrupted)
Average temperature along the main flow path: 350°C	Vessel heating system: not-active
Vessel heating system: not active	
HX Water flow rate: 0.5 kg/s	
DHR: not active	

In this work, the results obtained for two experimental tests are discussed. Table 4 shows the main parameters of the tests: duration, electrical power in FC and NC.

Table 4: Test Matrix

Test	***Duration of the test***	***Electrical Power***	
		FC	***NC***
I	48 h	730 kW	50kW
II	97 h	600 kW	23 kW

In Test I, the LBE level inside the tank is about 7850 mm (from the S100 internal bottom), which means approximately at mid-height of the DHR inlet slots. In Test II the LBE level is raised up to about 8000 mm from the S100 internal bottom, in such a way as to keep the slots completely flooded.

4. Experimental results

4.1 TEST I

Figure 17 (*a*) shows the power transient during the running of Test I. The experiment starts with nominal power of about 730 kW, and after 7 hours the transition to 50 kW. The primary LBE flow rate, which quickly reaches its nominal value, is about 56-57 kg/s (see Figure 17(*b*)); the strong oscillations in the first phase of the test shown in Figure 17(*b*), characterized by argon injection gas lift circulation, is related to the specific volumetric blowers used to inject the gas into the riser. After a few hours a check valve was put in service to dump such oscillations. After the gas injection switches off and the electrical power supply reduces to about 5% of nominal power, natural circulation conditions establish with the LBE flow rate that tend to about 7.5 kg/s (14% of the nominal flow rate).

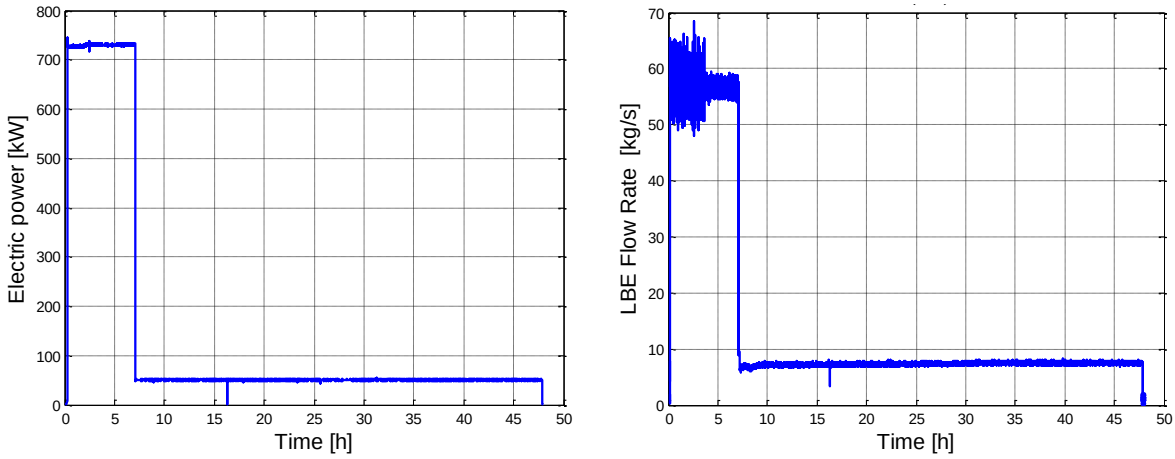

(*a*) (*b*)

Figure 17: Electrical power supplied to the FPS (*a*) and LBE flow rate through the primary system measured by the Venturi flow meter (*b*).

During the full power run, argon is injected into the riser to promote the main circulation along the primary system (gas flow rate of 1.8 Nl/s). After the transition from full power to "decay power", the gas injection was interrupted (see Figure 18 (*a*)) to simulate the station black-out, and transition from forced to natural circulation takes place. Argon mass flow rate revealed by the transducer after injection shutdown shows a value of 0.35 Nl/s, even if the argon line was completely closed due to the signal being at digital full scale (0.35-3.5 Nl/s). At full power run the HX is fed by water with a flow rate of 0.65 kg/s and water pressure at the inlet of the bayonet tubes (upward of the manifold) is close to around 2 bar. After station black-out simulation conditions the feedwater is closed and the water flow into the HX falls as shown in Figure 18(*b*). As can be noted in Figure 17 (*a*), after the transition from full power to "decay power" (about 16 hours after the start-up of the TEST-I) the electrical power decrease suddenly and then increase to the former value. This happen due to an actual blackout occurred on the power system (about 1 minute). Nevertheless, the short duration of the blackout and the great thermal inertia of the system are such as not to jeopardize the outcome of the performed test.

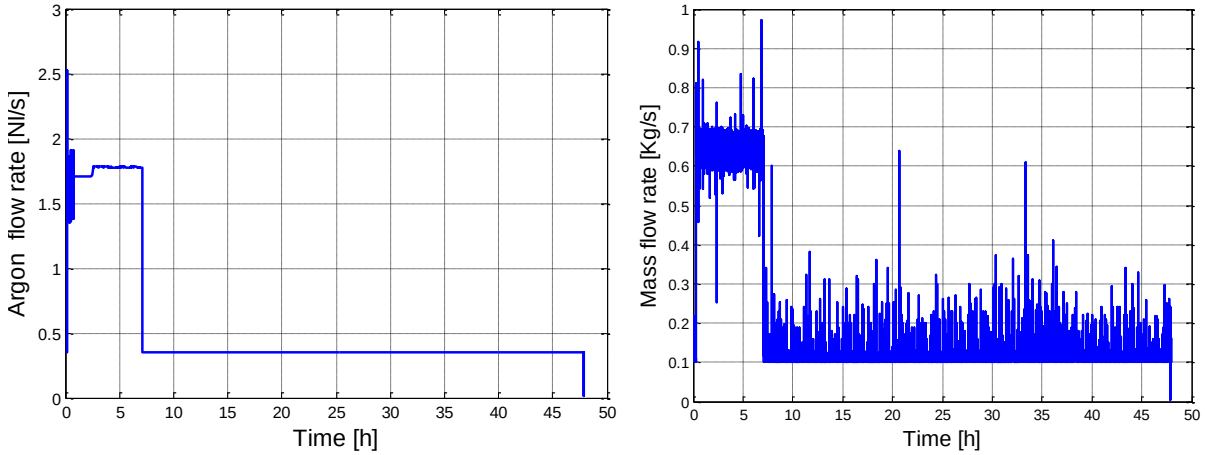

(*a*) (*b*)

Figure 18: Argon flow rate for the gas lift (*a*) and water mass flow rate in the HX (*b*)

After the “core scram”, in order to remove “decay heat” power, the DHR-system was activated; the air mass flow rate through the DHR was about 0.223 kg/s, as reported in Figure 19 (*a*).

Figure 19 (*b*)shows the average temperatures at inlet and outlet sections of the FPS. As can be noted, steady state conditions were achieved at full power after 4-5 hours of transients with a temperature difference between inlet and the outlet sections of about 77°C, the average inlet temperature being 285°C and the outlet average temperature 362°C.

At black-out simulation time, the average temperature at the FPS inlet decreases by about 5°C to a value of about 280°C, while the average temperature of the FPS exit decreases by 70°C reaching a value of about 295°C. Under natural circulation flow regime, the temperature difference along the FPS falls to around 24°C, being the average inlet and outlet temperature 349°C and the average outlet temperature of 373°C, at the end of the test. After a natural circulation transient of about 40 hours, the average temperature in the FPS still increases, and steady state conditions were not yet reached. This unbalance is essentially due to the fact the air mass flow rate flowing through the DHR system is not sufficient to remove more than 20-23 kW.

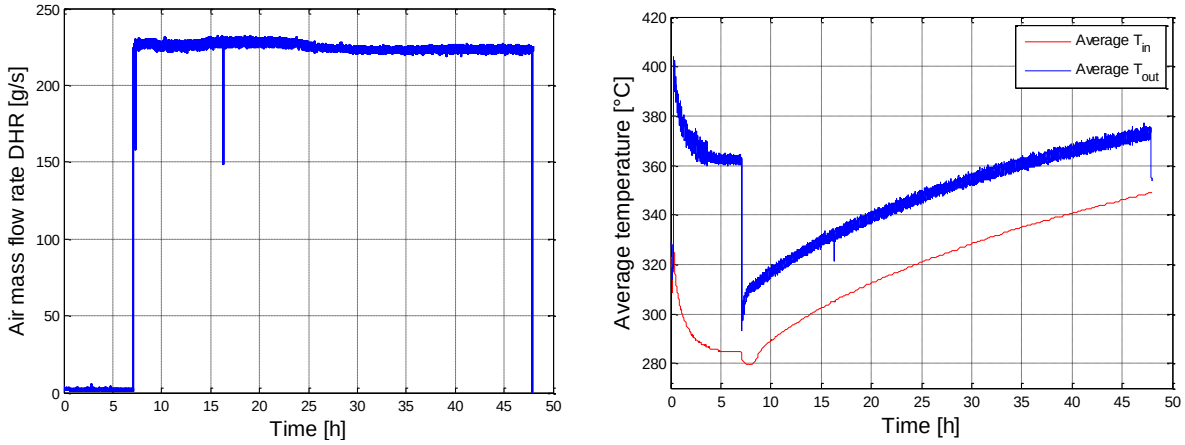

(*a*) (*b*)

Figure 19: Air mass flow rate through the DHR system (*a*) and average temperatures through the FPS (*b*)

Figure 20(*a*) and Figure 20(*b*) show the clad temperature of pin 1 and 7 associated with Inner sub-channels along the active length (for the position of the TCs see Figure 4 to Figure 7). After about 5 hours the temperature at Section 1 and 2 near the middle spacer grid reaches a constant value of about 380-390°C for pin 1 and 7 (T-FPS 4, 5, 10 and 11), while at section 3 the clad temperature for pin 1 (T-FPS 16) is about 20°C higher than the clad temperature of pin 7 (T-FPS 17, 410°C versus 430°C). This difference can be explained by looking at the pin manufacturing as reported in Figure 21. Due to the internal geometry adopted for the Bifilar-type pins, provided by Thermocoax, the thermal flux around the pins is not uniform. From Thermocoax technical documents, pin rods bifilar-type used in the ICE bundle, exhibit an approximate azimuthal variation of about 30%; therefore, the temperatures measured by the wall-pinched thermocouples can be higher or lower than the average wall temperatures. After the transition from forced to natural circulation, the clad temperatures increase both for pin 1 and 7, from a value of about 310 to 370°C (Section 1), from 320 to 380°C (Section 2) and from 330 to 395°C (Section 3).

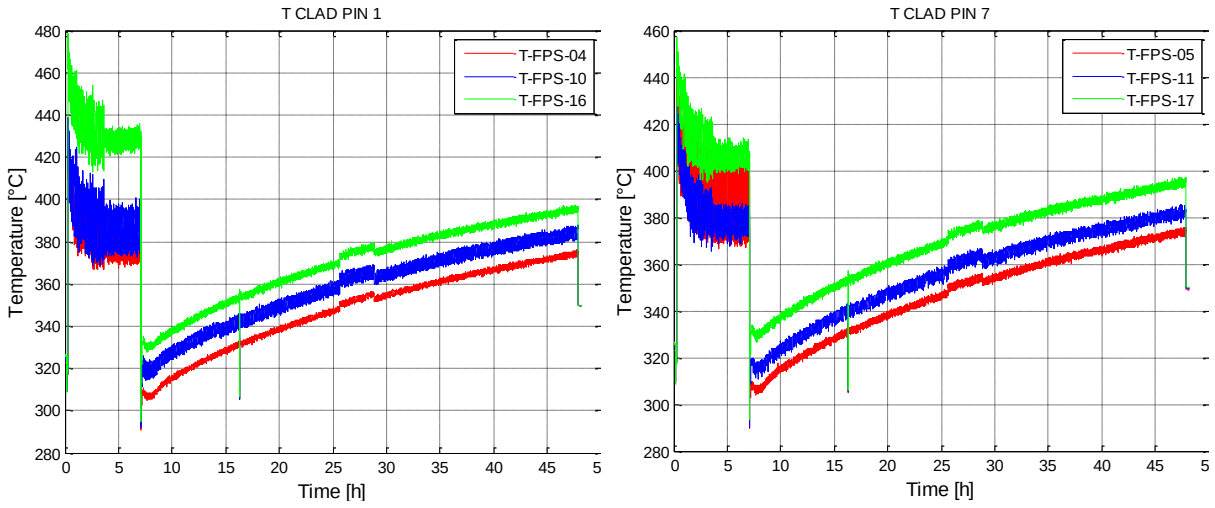

(*a*) (*b*)

Figure 20: Clad temperature pin 1 and 7 along the active length

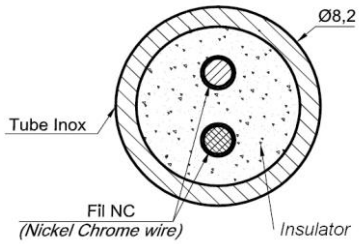

Figure 21: Cross section of the pin Bifilar-type (active zone)

Figure 22 (*a*) shows the temperature in the centre of the channel for the Inner sub-channel. Starting from Section 4 (T-FPS 30, 60 mm downstream of the lower spacer grid), the temperature at full power steady state condition reaches a value of about 280°C, it increases along the sub-channel reaching a value of about 320°C at Section 1 (T-FPS 01) and at Section 3 (60 mm upstream the upper spacer grid) the temperature value is about 365°C (T-FPS 24), hence the LBE flowing in the Inner sub-channel, from Section 4 to Section 3, increases its temperature by about 85°C. After the transition the temperature difference between the lower Section 4 and Section 3 is in the order of 40-45°C.

Tubes injecting argon below the molten metal level ("bubble tubes") have been installed to transfer pressure signals from the LBE alloy to differential pressure cells operating with gas at room temperature (accuracy ± 1 mm LBE see Ambrosini et al. 2004). During forced circulation condition, inlet and outlet pressure difference inside the riser is lower than that measured under natural circulation condition, essentially for the lower value of the two phase flow density compared to the LBE density. In particular, at full power steady state condition the pressure difference reaches a value of about 3420 mbar while, after the transition, the reached value is in the order of 3670 mbar. Then, it is possible to evaluate void fraction in the Riser of about 11% according to the work of Benamati et al. 2007. Therefore, the maximum available pressure head provided by the gas-lift system in the riser is around 430 mbar.

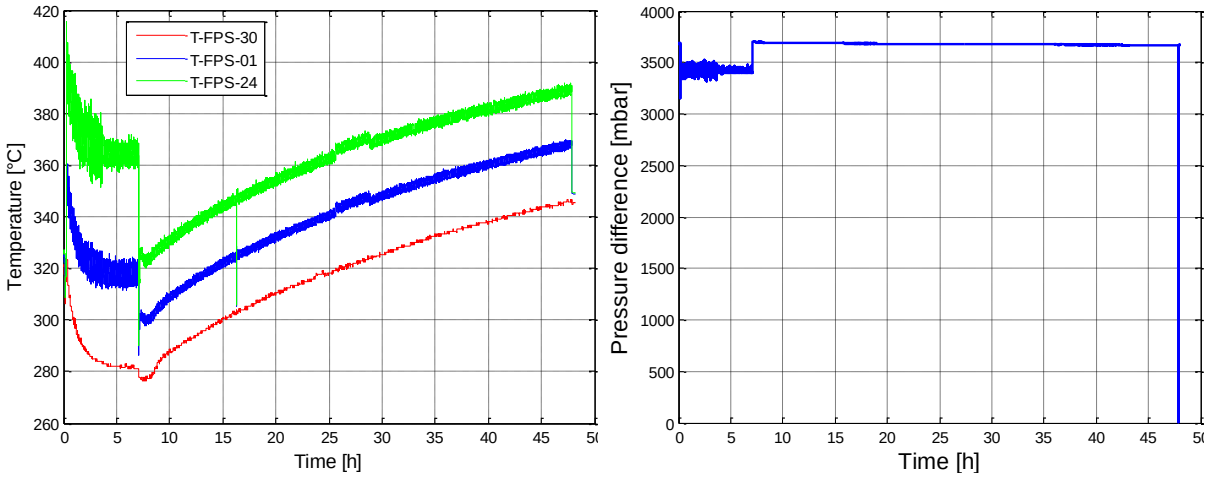

(*a*) (*b*)

Figure 22: Central sub-channel temperatures (*a*) and pressure difference between inlet and outlet section of the Riser(*b*)

Regarding temperatures in the sub-channels of the FPS at sections 1 and 3, Figure 23(*a*) and Figure 23(*b*) show the temperatures at the clad and centre of the channel for the central subchannel (uncertainty ~ ±0.1 °C). It must be stressed that, although the system is globally unbalanced in the 'DHR' phase with the average temperature growing with time, the heat transfer phenomena in the bundle are stationary, i.e. the temperature difference between wall and bulk remains constant.

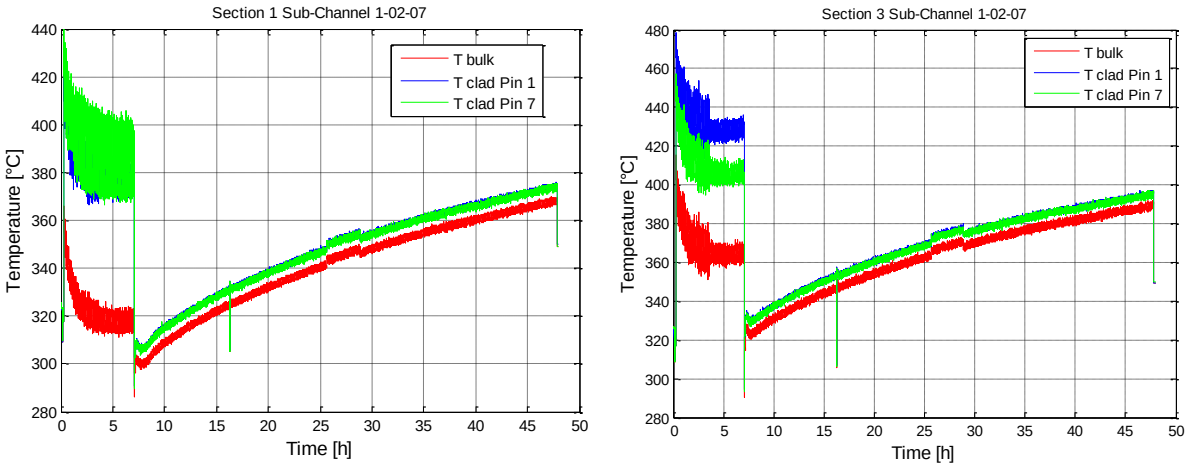

(*a*) (*b*)

Figure 23: Temperature measurement on the Central sub-channel at section 1 (*a*) and section 3 (*b*)

As already discussed for Figure 21, the clad temperature difference between pins 1 and 7 is due to the internal geometry adopted for the Bifilar-type pins. Assuming the temperature in the centre of the channel as the bulk temperature (being the only one measurable) the Nusselt number was evaluated as function of the Peclet number for the forced and natural circulation regime (see Figure 24). Obtained values underestimate Nu obtained from Ushakov and Mikytiuk correlations (Mikityuk 2009, Ushakov et al.1977) by less than 21 % at section 1 and 11% at section 3, respectively. Further investigation will be performed in order to obtain Nu number for the overall temperature range of interest.

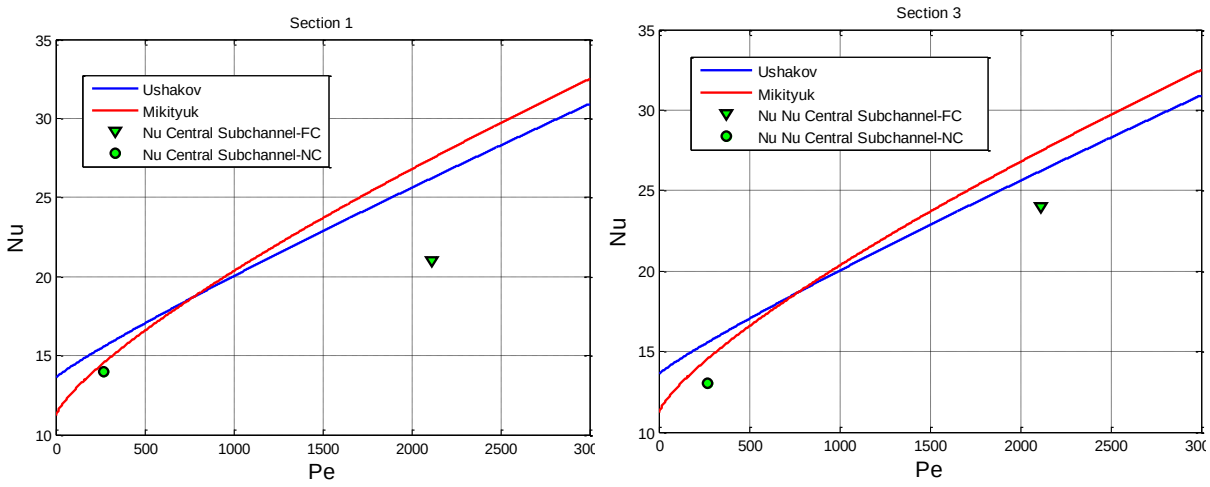

(*a*) (*b*)

Figure 24: Nusselt vs. Peclet number at Section 1 (*a*) and Section 3 (*b*)

From the riser exit, the LBE flows through the separator into the HX shell. Figure 25(*a*) and Figure 25(*b*) show HX inlet and outlet temperature, respectively.

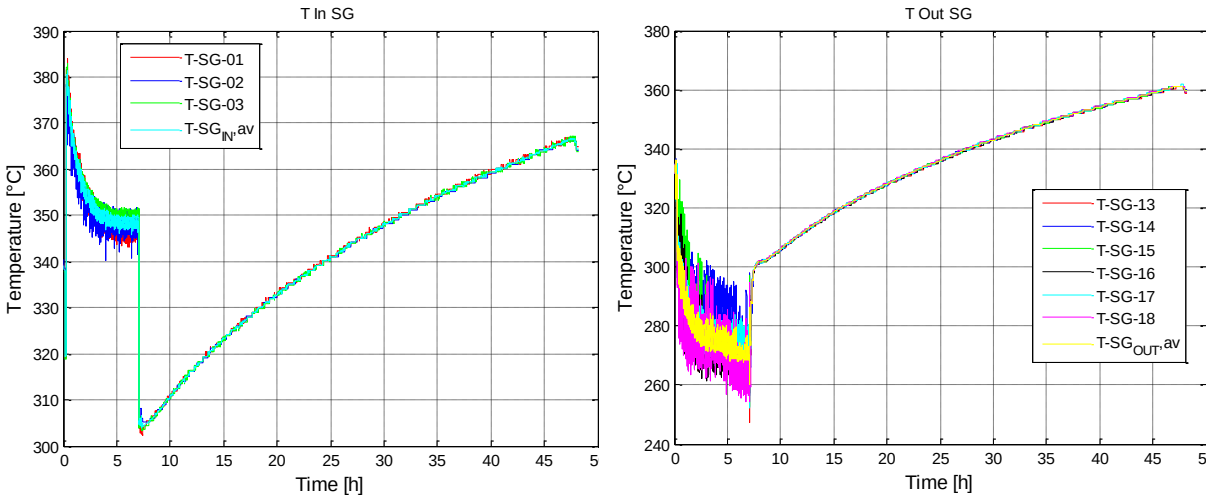

(*a*) (*b*)

Figure 25: LBE temperature at the entrance (*a*) and exit of the HX (*b*).

In full power steady state condition (when the HX is activated) the LBE temperature at the entrance of the HX is about 348°C, then through the HX the LBE exchanges heat with water of the secondary circuit decreasing its temperature by about 78°C reaching at the exit of the HX the value of about 270°C. Immediately after the transition to natural circulation the LBE enters the HX with a temperature of 305°C and exits with a temperature of 301°C, while at the end of the experiment the LBE temperature at the HX inlet section is about 366°C. The temperature drop between the HX inlet and outlet section under natural circulation conditions is 4-5 °C and it is mainly due to heat losses toward the LBE external pool. In steady state full power conditions the thermal power removed by the HX is in the order of 640 kW. Considering energy balance for the steady state at full power run, the difference between the supplied energy and the power removed by the HX is about 90 kW (see Figure 26 (*a*)).

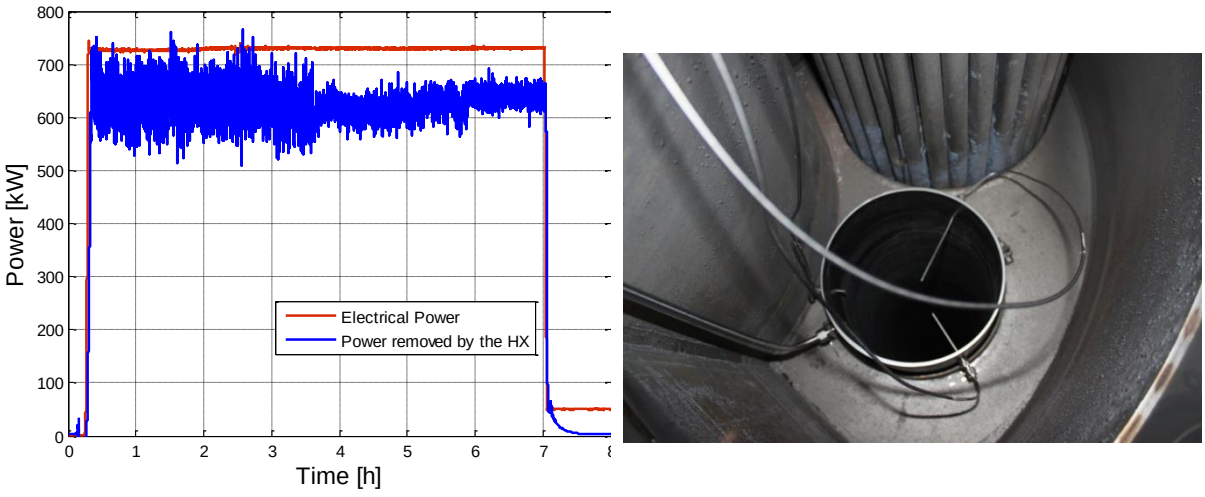

(a) *(b)*

Figure 26: Energy balance at full power run

The difference between electrical power supplied to the FPS and the thermal power removed by the HX in full power steady state condition is essentially due to:

- About 5% of the supplied electrical power is converted to heat in the electrical cable for Joule effect and removed by Insulation Volume Cooling System IVCS (Bandini et al. 2001);
- The calculation does not take into account the power removed by the HX tubes inside the separator before the inlet in the HX pipe where TCs are placed (see Figure 26(*b*));
- Heat losses towards the external environment.

Inside the external LBE pool, several thermocouples were installed in order to investigate mixing and stratification phenomena (see Figure 16). Figure 27 and Figure 28 show the temperature inside the LBE pool along the 8 different vertical lines (see Figure 15). In particular, TCs on lines *A, H, I* allow measurement from the upper section (0 mm in Figure 16) to the FPS entrance level (-7200 mm), while TCs on lines *B, C, D, E, F, G* allow measurement up to 600 mm below the exit of the DHR.

Observing the experimental data, results show that the LBE temperature is homogenous at each horizontal section.

The temperature in the pool (320-330°C) at the beginning of the experiment (0.3 h), is quite uniform vertically, changing about 10°C from the first upper TC and the bottom one (7.2 m lower than the first TC, see Figure 27 (*a*)). At this time the electrical power ramp is at one third of its maximum power, the DHR is not activated and the argon mass flow rate is 1.78 Nl/s. After about 6 h (see Figure 27(*b*)), just before transition to natural circulation, with thermal power at steady state condition and a constant Argon mass flow rate, the LBE temperature in the lower region of the pool is at its coldest value assuming a uniform temperature of about 283°C. Between the exits of the DHR and the HX, respectively 4.2 and 3.6 m, a thermal stratification phenomenon with a temperature variation of about 17°C can be observed. In the upper part of the plenum then the temperature increases reaching a value of about 340°C.

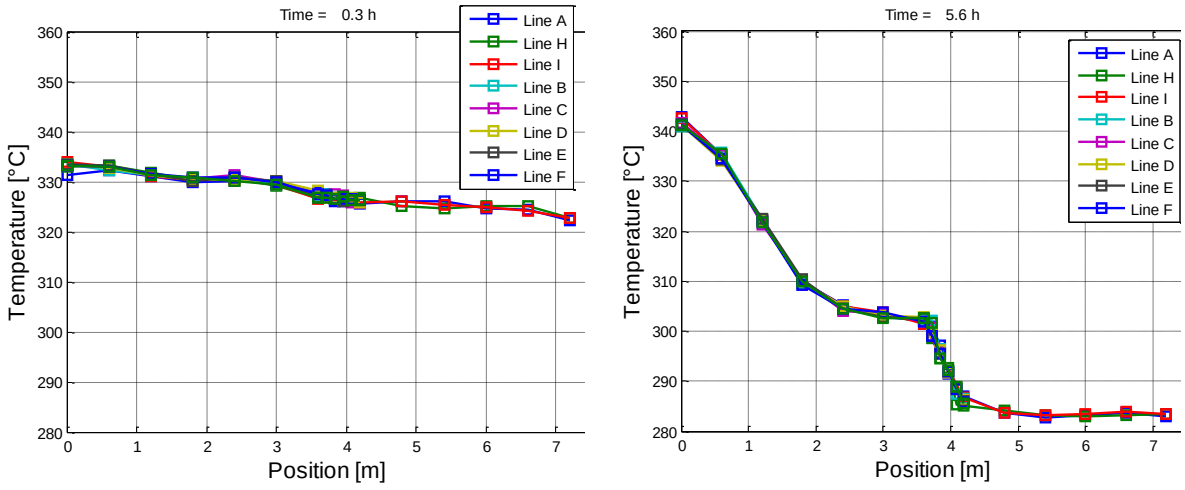

(*a*) (*b*)

Figure 27: Temperature of the LBE inside the pool at t = 0.3 h (*a*) and at t = 5.6 h (*b*)

After the transition from forced to natural circulation, the supplied electrical power is reduced to 50 kW, the secondary air system in the DHR is activated and the Argon injection in the riser is stopped. At *t* = 7.8 h the LBE temperature in the upper plenum became uniform assuming a value of about 300°C, the region where thermal stratification phenomena are significant moves downwards starting from the DHR outlet section (4.2 m, see Figure 28 (*a*)) up to about 4.8 m; the temperature difference between these two sections is about 17-20°C.

In the lower plenum of the pool the LBE temperature is quite uniform showing a value of about 280°C. From *t* = 7.8 h to *t* = 47.8 h (see Figure 28(*b*)), temperatures in the pool gradually rise, reaching, the end of the experiment, at value of about 360°C in the upper plenum of the pool and about 350 °C in the lower plenum (steady state condition not yet reached). The temperature difference, in the area where thermal stratification phenomena are relevant, comes down to a value of about 10°C.

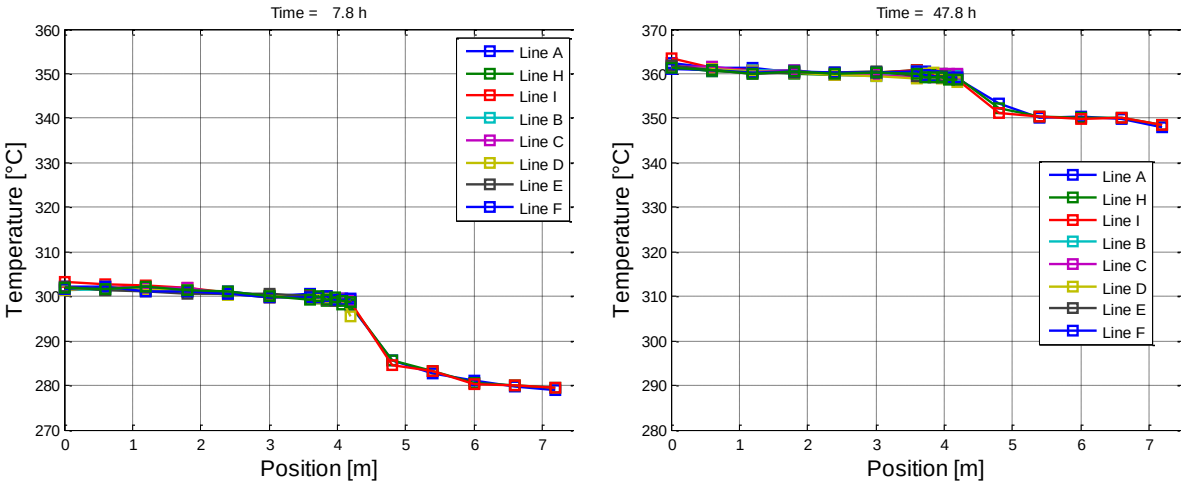

(*a*) (*b*)

Figure 28: Temperature of the LBE inside the pool at t = 7.8 h (*a*) and at t = 47.8 h (*b*)

4.2 TEST II

This test was performed reducing the power supplied to the FPS both during forced and natural circulation conditions with respect to the previous test with the aim of reaching a steady state temperature trend under natural circulation conditions with decay heat removed by the DHR system. During the full power run of Test II, electrical power supplied to the FPS was about 600 kW. After the transition it was reduced to 40 kW (Figure 29(*a*)). The argon flow rate was set to about 5.2 Nl/s and the obtained LBE mass flow rate in the FPS measured by the Venturi flow meter is in the order of 63-64 kg/s. After the transition to natural circulation the LBE mass flow rate in the FPS reached a value of about 8.5 kg/s (Figure 29(*b*)).

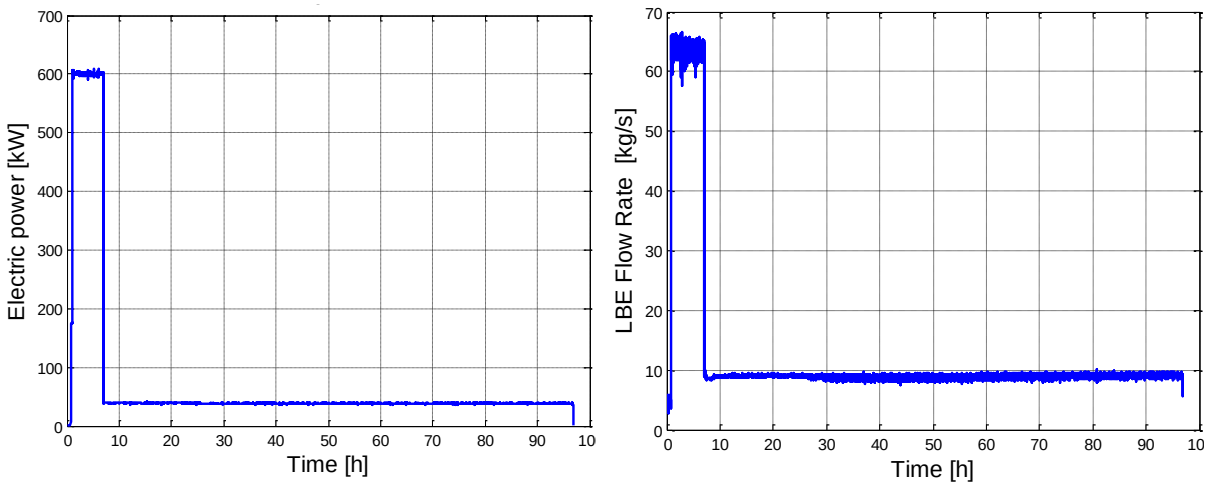

(*a*) (*b*)

Figure 29: Test II, electrical power supplied to the FPS (*a*) and LBE flow rate through the primary system measured by the Venturi flow meter (*b*).

The secondary water circuit was fed by water with a flow rate of 0.5 kg/s and the thermal power removed by the HX, evaluated from an energy balance on LBE side, was about 530 kW. The duration of the full power run is about 7 h, after that the transition to decay heat removal under natural circulation condition took place and the DHR was activated. The power imposed to be removed by the DHR-system was 20 kW and after about 25 h it was increased to about 23 kW (Figure 30).

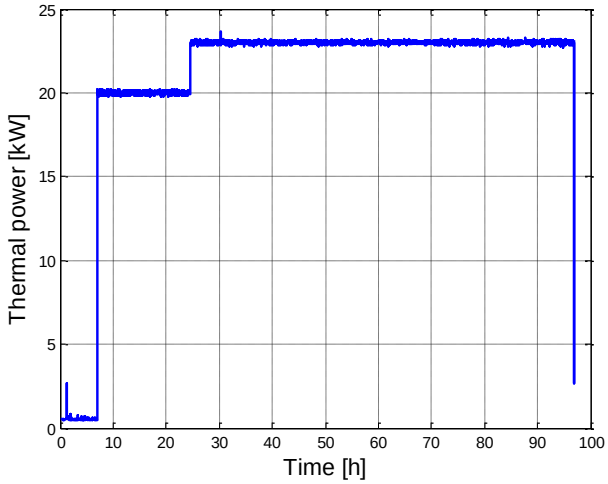

Figure 30: Thermal power removed by the DHR-system

Through the FPS the LBE increased its temperature of about 60°C at full power run and after the transition the difference in temperature reduced to about 21°C (Figure 31(*a*)). The difference in temperature between the inlet and outlet sections of the water heat exchanger was about 52°C at the end of the full power run, while he temperature drop in the HX under natural circulation condition was about 4°C and it was mainly due to heat losses toward the LBE external pool (Figure 31 (*b*)).

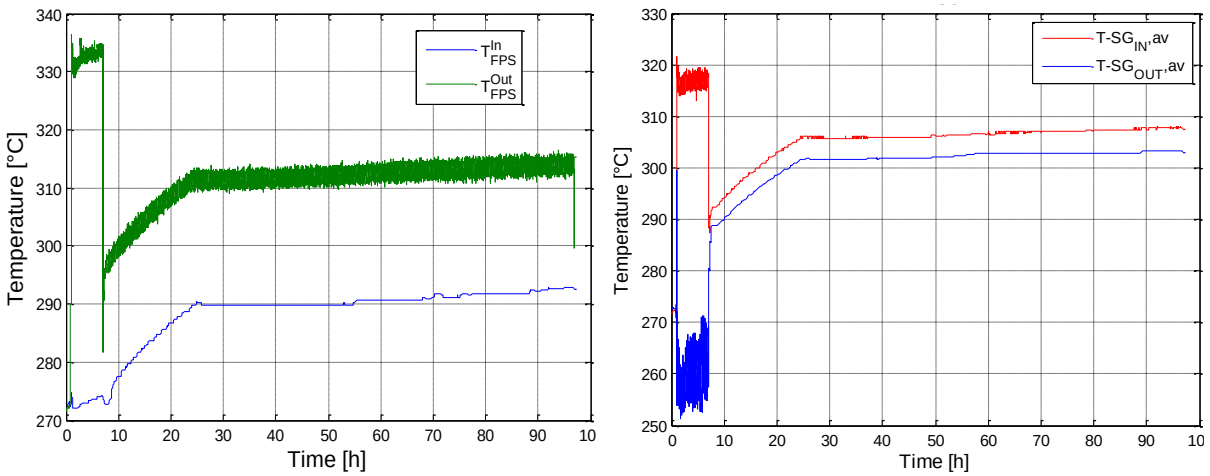

(*a*) (*b*)

Figure 31: Average temperatures through the FPS (*a*) and through the steam generator (*b*)

The same considerations introduced in Test I can be applied to Test II in order to explain the difference between electrical power supplied to the FPS at full power run and the power removed by the HX (see Figure 32). After transition to natural circulation condition the external heat losses at steady state conditions are in the order of about 17 kW.

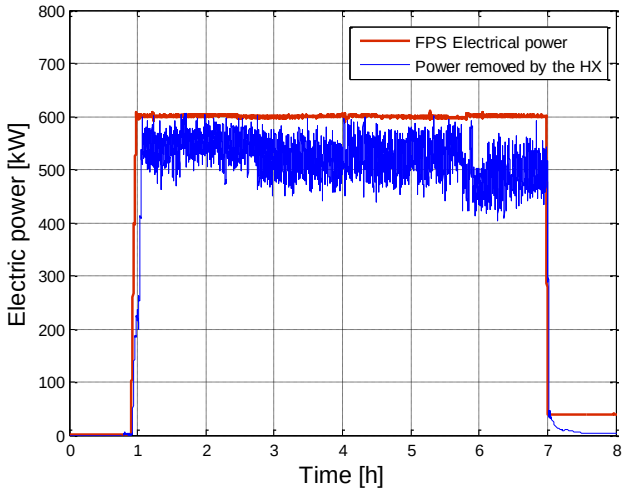

Figure 32: Energy balance at full power run

According to the obtained temperature in the central sub channel (error ~ ±0.1 °C) for section 1 and 3 (see Figure 33) the Nusselt number was evaluated assuming the temperature at the centre of the sub channel to be the bulk temperature.

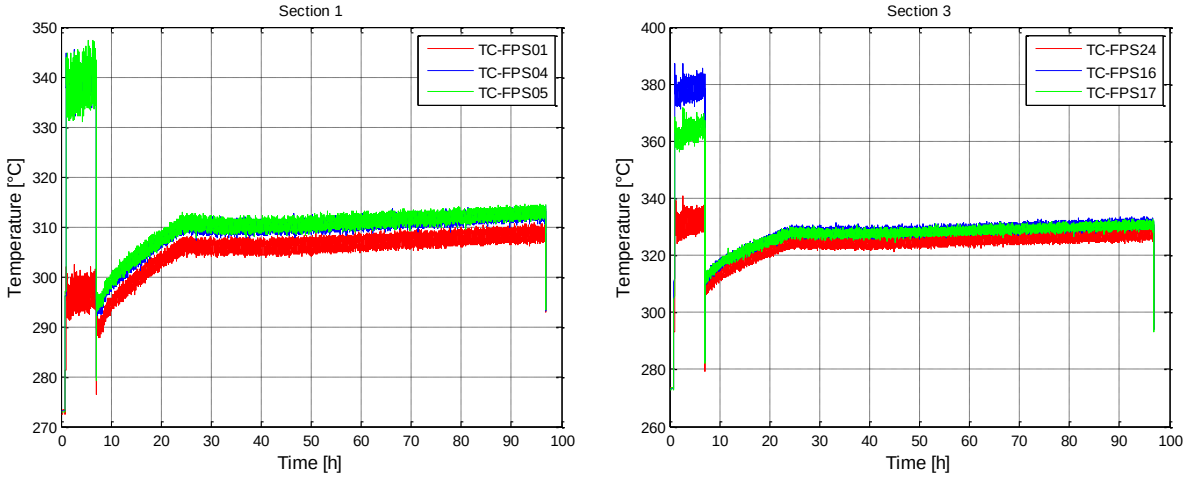

(*a*) (*b*)

Figure 33: Temperature measurement on the Central sub-channel at section 1 (*a*) and section 3 (*b*)

Calculated Nusselt numbers (see Figure 34) differ from Ushakov and Mikityuk's correlation by less than 28%, further dedicated tests will be performed in order to characterize the heat exchange in fuel bundles.

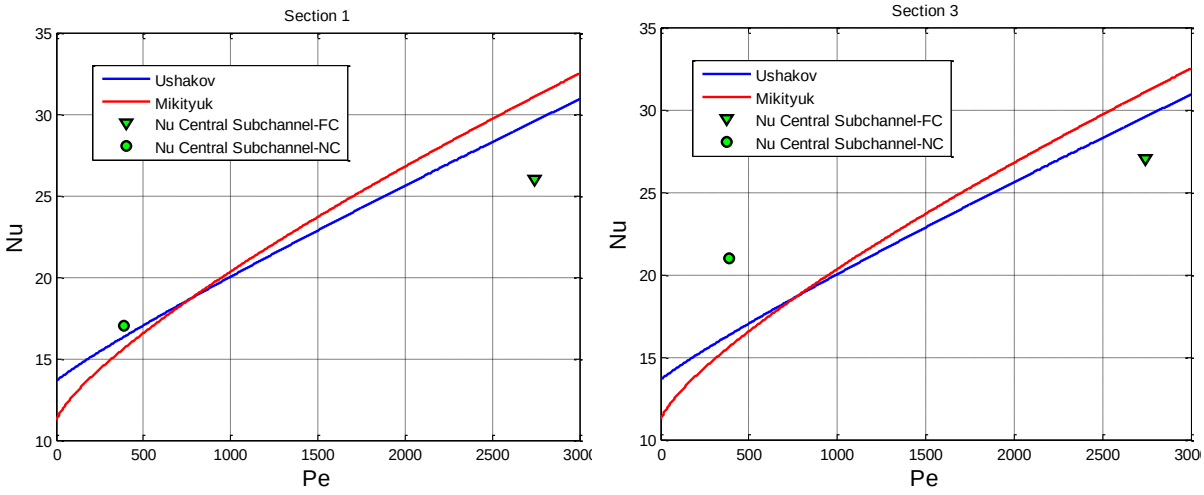

(*a*) (*b*)

Figure 34: Nusselt vs. Peclet number at Section 1 (*a*) and Section 3 (*b*)

Concerning temperatures inside the CIRCE pool, at the beginning of the test temperatures are uniform assuming a value of about 272 °C (see Figure 35(*a*)). After about 6 h (see Figure 35(*b*)), before transition to natural circulation the behaviour is analogous to what was found for Test I. After transition to natural circulation, the region where thermal stratification phenomena are significant moves downwards starting from the DHR outlet section (4.2 m) up to about 4.8 m. The temperature difference between the upper and lower plenum is about 10-12°C. The stratification in the pool reached a steady state condition after about 30 h maintaining the same profile up to the end of the experiment (see Figure 36 (*a*) and (*b*)).

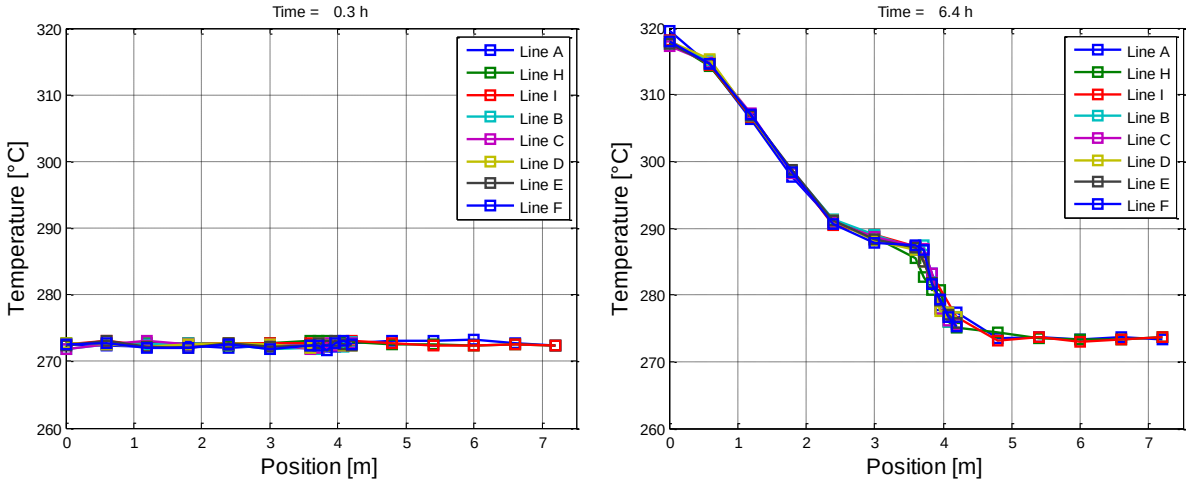

(*a*) (*b*)

Figure 35: Temperature of the LBE inside the pool at t = 0.3 h (*a*) and at t = 6.4 h (*b*)

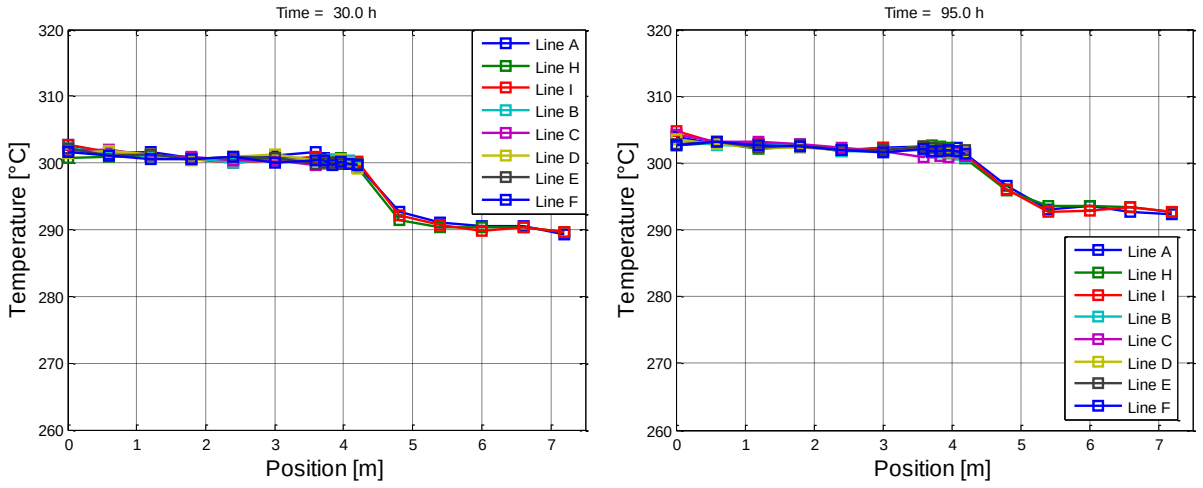

(*a*) (*b*)

Figure 36: Temperature of the LBE inside the pool at t = 30 h (*a*) and at t = 95 h (*b*)

5. Conclusions and Outlook

In the frame of HLM technology development supporting the LFR/ADS nuclear system design and operation, the CIRCE pool facility was refurbished to host a suitable test section to simulate the thermal-hydraulic behaviour of a HLM cooled pool reactor primary system.

In particular, a fuel pin bundle simulator (FPS) was installed, coupled with a main heat exchanger, a decay heat removal system and a gas lift system in order to sustain the forced circulation.
In the present work, results related to experiments reproducing a PLOHS+LOF accident, are reported, i.e. Test I (48 h) and Test II (97 h). Both tests simulate the transition from forced to natural circulation typical of the Decay Heat Removal scenario in a HLM pool-type reactor. Test II was performed reducing the thermal power supplied to the FPS both under forced and natural circulation with the aim of reaching a steady state temperature trend under natural circulation conditions.
Performed tests are of great interest for both the mixing and stratification phenomena and for local heat transfer in the pin bundle. During the tests, mixed convection phenomena through the FPS were analysed monitoring the bulk and cladding temperature in instrumented sections.

For Test I, during forced circulation phase, the electrical power supplied is 730 kW and the LBE mass flow rate in the FPS is about 56-57 kg/s. In this condition, the average velocity in the bundle is around 1.0 m/s and the Nusselt number, averaged between section 1 and section 3, is estimated to be around 20-25. Thereafter, the electrical power supplied to the bundle is reduced to 50 kW (7% of the full power) and the LBE mass flow rate through the FPS decreases by 87% under natural circulation regime. In this condition, the averaged Nusselt number is estimated to be around 14-16.

For Test II, the electrical power supplied to the FPS during full power regime, is 600 kW and the LBE mass flow rate in the bundle is about 63-64 kg/s. After the simulation of the accidental scenario the electrical power supplied to the bundle is reduced by 7% of the full power (40 kW) and the LBE mass flow rate through the FPS decreases by 87% under natural circulation condition.

Concerning the thermal stratification inside the pool at full power steady state condition, a similar behaviour is observed both for Test I and Test II. Both tests started with a uniform temperature in the pool, around 320°C-330°C for Test I and 270°C for Test II. During the tests, temperature decreases by about 40°C from the upper part of the pool to the outlet section of the heat exchanger.
The vertical thermal gradient is mainly localized in the region between the outlet sections of the HX and the DHR, with a temperature drop of about 20°C. Moreover, the experimental evidence shows that thermal stratification in the pool is purely vertical with negligible temperature variation on the horizontal planes. After transition to natural circulation, the region where the thermal gradient is localized moves downwards starting at the exit section of the DHR-system and is characterized by a temperature drop of about 10°C.
Especially in Test I the global thermal unbalance in DHR condition leads the average temperature of the system gradually to increase, but this does not alter the temperature gradients.

The experiments performed in the CIRCE large pool lead to a preliminary demonstration of the technological feasibility of a HLM primary system nuclear reactor, investigating the pool behaviour under nominal and transient conditions.
The gained results shown the favourable behaviour of a LFR during a long term station blackout, allowing to fully characterize the decay heat removal scenario, both in term of flow rate and flow paths, temperature fields and in term of transient behaviour, highlighting the constants of time which characterize a heavy liquid metal large pool.
Moreover, the thermal stratification (or the lack of mixing in the downcomer) observed during the tests will pose significant issues to be faced by the system designer.
From one side, induced thermal-fatigue stresses need to be accounted during the design phase, considering the expected magnitude and axial slope.
On the other hand, the oxygen distribution in the coolant is strongly affected by the thermal stratification, posing relevant issues related to the coolant chemistry control and corrosion of structural materials in the pool.

Finally, gained experimental data on mixed convection and thermal stratification, are valuable in supporting the validation of both the thermal-hydraulic system code and the CFD code (and their coupling) when employed on HLM large pools.
Further experimental tests are needed in order to further understand the involved phenomena and fully investigate pool behaviour.

Acknowledgements

This work would not have been possible without the EC financial support in the frame of the Collaborative Project THINS, Grant agreement No 249337. The authors gratefully acknowledge the work done by the staff of the thermal-fluid-dynamic and facility operation by the experimental engineering technical unit of Brasimone (UTIS-TCI) for the operation of CIRCE facility.

References

Agostini, P., Alemberti, A., Ambrosini, W., Benamati, G., Bertacci, G., Cinotti, L., Elmi, N., Forgione, N., Oriolo, F., Scaddozzo, G., Tarantino, M., "*Testing and qualification of CIRCE Venturi-Nozzle flow meter for large scale experiments*" 13th International Conference on Nuclear Engineering, Beijing, China, May 16–20, 2005.

Alemberti A, Smirnov V., Smith C.F., Takahashi M., "*Overview of lead-cooled fast reactor activities*", Progress in Nuclear Energy, article in press.

Ambrosini W., Azzati M., Benamati G., Bertacci G., Cinotti L., Forgione N., Oriolo F., Scadozzo G., Tarantino M., "*Testing and qualification of CIRCE instrumentation based on bubble tubes*", Journal of Nuclear Materials, pp. 293-298, 2004.

Artioli C., "*Specification for the EFIT Core and Fuel Element Design*", Deliverable D. 1.6, DM1 DESIGN, IP-EUROTRANS, 2006.

Bandini G., Di Piazza I., Gaggini P., Del Nevo A., Tarantino M., "*CIRCE experimental set-up design and test matrix definition*", ENEA UTIS-TIC Technical Report, IT-F-S-001, 28/02/2011.

Barbensi A., Corsini G., "*Specification for the EFIT primary system*", Deliverable D. 1.4, DM1 DESIGN, IP-EUROTRANS, 2006.

Benamati G., Bertacci G., Elmi N., Scaddozzo G., "*Report on Gas Enhanced Circulation Experiments and Final Analysis (TECLA D41)*", Report ENEA HS-A-R-016, 2005.

Benamati G., Foletti C., Forgione N., Oriolo F., Scadozzo G., Tarantino M., "*Experimental study on gas-injection enhanced circulation performed with the CIRCE facility*" Journal of Nuclear and Engineering Design, 237, pp. 768-777, 2007.

De Bruyn D., Mansani L., Giraud B., "*From MYRRHA to XT-ADS: The Design Evolution of an Experimental ADS System*", AccApp'07, Pocatello,Idaho,July 29-August2, 2007.

Cinotti L., Tarantino M., Rozzia D., "*Lead-cooled Fast Reactor development Gaps*", IAEA Technical Meeting on to Identify Innovative Fast Neutron Systems Development Gaps, IAEA Headquarters, 29 February – 02 March 2012, Vienna, Austria. (http://www.iaea.org/NuclearPower/FR/).

Foletti C., Scadozzo G. Tarantino M., Gessi A., Bartacci G., Agostini P., Benamati G., "*ENEA experience in LBE technology*", Journal of Nuclear Material, 356 pp. 264-272, 2006.

Giraud B., "*Review and justification of the main design options of XT-ADS*", Deliverable D. 1.5, DM1 DESIGN, IP-EUROTRANS, 2006.

Ishitori T., Ogura K., Sato K., Oshima I., Nei H., Uotani M., Fukada T., Akimoto T. "*Experimental study of sodium natural convection heat transfer in the intermediate plenum for pool-type LMFBRs*", Nuclear Engineering and Design, Vol 99, pp. 431-440, 1987.

Mansani L., "*Candidates Materials for XT-ADS and EFIT, Operating Conditions and Testing Requirements*", Deliverable D. 4.1, DM4 DEMETRA, IP-EUROTRANS, 2005.

Mikityuk K., "*Heat transfer to liquid metal: review of data and correlations for tube bundles*", Nuclear Engineering and Design, Vol. 239, 680–687, 2009.

Sustainable Nuclear Energy Technoloy Platform, "*A Contribution to the EU Low Carbon Energy Policy: Demonstration Programme for Fast Neutrron Reactors*",ESNII Concept Paper, 2010.

Seventh Framework Programme FP7, http://cordis.europa.eu/fp7/home_en.html, 2014.

Tarantino M., Scaddozzo G., "*Test specifications of the Integral Circulation Experiments*", Report ENEA ET-F-S-001, Deliverable D. 4.15, DM4 DEMETRA, IP-EUROTRANS, 2006.

Tarantino M., Agostini P., Benamati G., Coccoluto G., Gaggini P., Labanti V., Venturi G., Class A., Liftin K., Forgione N., Moreau V., "*Integral Circulation Experiment: Thermal-hydraulic simulator of heavy liquid metal reactor",* ", Journal of Nuclear Materials, 415, pp. 433-448, 2011.

Turroni P., Cinotti L., Corsini G., Mansani L., "*The CIRCE Facility*", AccApp'01&ADTTA'01, Nuclear Application in the new Millennium, Reno (Nevada- USA), November 11-15, 2001.

Ushakov P.A., Zhukov A.V., Matyukhin M.M., "*Heat transfer to liquid metals in regular arrays of fuel elements, High Temperature*", Vol. 15, pp. 868–873, 1977; translated from Teplofizika Vysokikh Temperatur 15 (5), pp. 1027–1033, 1977.

Van den Eynde G.,"*Specification for the XT-ADS Core and Fuel Element Design*", Deliverable D. 1.7, DM1 DESIGN, IP-EUROTRANS, 2007.

Watanabe O., Motomiya Y., Takeda H., Koga T. "*An application of higher order finite difference method to a natural convection experiment in the hot plenum of an LMFBR*", Nuclear Engineering and Design, Vol 146, pp. 25-34, 1994.